



**HAL**  
open science

## Laser Switching and Sorting for High Speed Digital Microfluidics

Matthieu Robert de Saint Vincent, Régis Wunenburger, Jean-Pierre Delville

► **To cite this version:**

Matthieu Robert de Saint Vincent, Régis Wunenburger, Jean-Pierre Delville. Laser Switching and Sorting for High Speed Digital Microfluidics. Applied Physics Letters, 2008, 92, pp.154105 (1-3). 10.1063/1.2911913 . hal-00389849

**HAL Id: hal-00389849**

**<https://hal.science/hal-00389849>**

Submitted on 29 May 2009

**HAL** is a multi-disciplinary open access archive for the deposit and dissemination of scientific research documents, whether they are published or not. The documents may come from teaching and research institutions in France or abroad, or from public or private research centers.

L'archive ouverte pluridisciplinaire **HAL**, est destinée au dépôt et à la diffusion de documents scientifiques de niveau recherche, publiés ou non, émanant des établissements d'enseignement et de recherche français ou étrangers, des laboratoires publics ou privés.

# Laser Switching and Sorting for High Speed Digital Microfluidics

Matthieu Robert de Saint Vincent<sup>†</sup>, Régis Wunenburger, and Jean-Pierre Delville<sup>\*</sup>

Université Bordeaux I, Centre de Physique Moléculaire Optique et Hertzienne, UMR CNRS 5798, 351

Cours de la Libération, F-33405 Talence cedex, France

**Abstract:** We used thermocapillary stresses induced locally by laser on flowing drops to build high throughput drop switchers and sorters for digital microfluidics. Since the laser is disconnected to the chip, the method does not require dedicated micropatterning. We show switching efficiencies of *100%* for drop velocities up to *1.3 cm/s*, demonstrate the involved mechanism and apply laser switching for sorting droplets of different nature for lab-on-a-chip applications.

PACS Numbers: 42.62.-b, 47.61.-k, 47.55.dm

---

<sup>†</sup> E-mail address: m.st-vincent@cpmoh.u-bordeaux1.fr

<sup>\*</sup> E-mail address: jp.delville@cpmoh.u-bordeaux1.fr

Droplet microfluidics, also called digital microfluidics, is now recognized as a revolutionary technique for managing high-throughput massively multiplexed arrays of chemical microreactors or biological assays with small quantities of reagents.<sup>1</sup> However, as soon as fast flowing nanoliter droplets are used as tight fluid reactors or carriers, new reliable fluid-handling micro-technologies are required to handle accurately these droplets within the robust environment of microchannels. While the geometry is able to manage drop formation through flow focusing<sup>2</sup> or T junctions,<sup>3</sup> challenges still remain for controlling droplet traffic. For instance, sorting needs an external forcing. Different approaches were proposed, involving mechanical,<sup>4</sup> electric,<sup>5</sup> optical,<sup>6</sup> and thermal<sup>7</sup> actuation. Two techniques are nevertheless able to manage high droplet velocities: digits were thermally switched at flow velocities of the order of  $2-3 \text{ mm/s}$ <sup>8</sup> and dielectrophoretically sorted up to  $3 \text{ cm/s}$ .<sup>9</sup> Nonetheless, these sorters need dedicated micropatterning for implanting local heating sources and electrodes, thus preventing further spatial and real-time reconfiguration of the external forcing.

In this Letter, we propose an alternative where the forcing fulfills these requirements. It is based on laser-induced localized thermocapillary stresses on the interface of flowing droplets (also known as Marangoni effect<sup>10</sup>) and allows for controlled high throughput sorting. Exploiting the fact that thermocapillary forces of the  $\mu\text{N}$  range are produced with low power lasers,<sup>11</sup> we demonstrate switching efficiencies of  $100\%$  for drop velocities up to the  $\text{cm/s}$  and illustrate the ability of laser switching for sorting different type of droplets in lab-on-a-chip devices.

The experiment consists in focusing a continuous TEM<sub>00</sub> Argon-Ion laser (wavelength in vacuum  $\lambda_0 = 514.5 \text{ nm}$ ) on a Polydimethylsiloxane (PDMS) microchannel using an inverted microscope. Water and Hexadecane, called hereafter oil, are pumped at constant flow rates  $Q_w$  and  $Q_o$ .  $2\% \text{ wt}$  Span 80, a

surfactant, is added to the oil. As illustrated in Figure 1, water droplets are formed at a T junction (not seen) in a central channel ( $100 \mu\text{m}$  wide) and travel downstream towards an enlarged Y junction ( $400 \mu\text{m}$  wide) ended by two opposite exit channels ( $200 \mu\text{m}$  wide); the channel height is  $h = 30 \pm 5 \mu\text{m}$ . The beam, of power  $P$ , is focused inside the enlarged channel using a microscope objective of magnification  $\times 2.5$  to form a beam waist  $\omega_0 = 10.3 \mu\text{m}$ . Flowing water drops are locally heated with the laser by adding  $0.1\%$  wt of fluorescein (optical absorption of the aqueous solution  $\alpha = 1.18 \text{ cm}^{-1}$ ). Finally, the droplet traffic is digitized with a high speed CMOS camera. Experiments were performed for nine couples of oil/water flow rates, to vary the radius  $R$  ( $54 - 70 \mu\text{m}$ ) and the mean droplet velocity at beam location  $U$  ( $0.6 - 13.0 \text{ mm/s}$ ).

A typical experiment is presented in Figure 1. Without laser, water drops formed upstream arrive in the enlarged part of the Y junction and flow asymmetrically downstream towards the exit channel of smaller hydrodynamic resistance (the down one in pictures). This weak asymmetry is forced by shortening one of the outlets, as in Ref. 9. Conversely, when a flowing drop is shined below its equator by the laser, it is suddenly pushed out towards the opposite direction. Figure 1 shows this switching process for different drop velocities  $U$  up to  $1.3 \text{ cm/s}$ .

To explain this effect, not observed with pure water drops (see below), we assume that local laser heating induces interfacial tension gradients which produce in turn a net thermocapillary force on the drop whose behavior is imposed by the sign of the rate of change of interfacial tension with temperature ( $\partial\sigma/\partial T$ ). In our system,  $(\partial\sigma/\partial T) > 0$  due to the large concentration in surfactant,<sup>12</sup> yielding to a thermocapillary force that pushes drops away from the beam. Consequently, as far as the heat diffusion time  $h^2/D_T$  ( $\approx 6 \text{ ms}$ ), where  $D_T$  is the thermal diffusion, and the viscous time  $\rho h^2/\eta$  ( $\approx 1 \text{ ms}$ ) required to trigger Marangoni flows are smaller than or of the order of the flowing time  $R/U$  ( $\approx 6 \text{ ms}$ , for  $R \approx 60 \mu\text{m}$ ,

$U \approx 1 \text{ cm/s}$ ), the beam behaves as an active wall whose stiffness is actuated by the exposure. The beam power effect on the drop center of mass is illustrated in the left Inset of Figure 2. It appears a deviation in drop trajectory which sharply increases with  $P$ .

According to Ref 13, the thermocapillary migration of a flat drop in a Hele-Shaw cell at low Reynolds and Marangoni numbers behaves as in unconfined liquid matrices

$$\langle \vec{U}_{Th} \rangle = -\frac{2}{2\eta_o + 3\eta_w} \left( \frac{\partial \sigma}{\partial T} \right) \frac{R}{2 + \Lambda_w / \Lambda_o} \vec{\nabla} T, \text{ where } \eta_{o,w} \text{ are shear viscosities and } \Lambda_{o,w} \text{ thermal}$$

conductivities), although the amplitude of the velocity is slightly reduced by wall friction. Then,

considering the maximum thermal gradient induced by the laser absorption  $|\vec{\nabla} T|_{Max} \propto P/\omega_o$ ,<sup>14</sup> the mean thermocapillary velocity should scale as  $\langle U_{Th} \rangle \propto RP$  in our enlarged chamber, all other variables held constant. To check this scaling, (i) we vary the drop radius  $R$  by changing the couple of water/oil flow rates, and (ii) for each couple we measure variations of the drop velocity in  $x$  and  $y$  directions with beam power. Figure 2 shows these velocity components for the drop trajectory at  $P = 53mW$  illustrated in the left Inset. By subtracting the drop velocity without laser (also shown in Figure 2), we finally get the mean velocity change  $\langle U_{Th} \rangle$  at given beam power and drop radius. This data analysis is iterated at different beam powers for the nine couples of flow rates investigated. The right Inset of Figure 2 shows the resulting variation of  $\langle U_{Th} \rangle$ . The expected linear behavior in  $RP$  is retrieved, thus demonstrating the mechanism of droplet switching. Furthermore, the thermocapillary migration amplitude

$$\langle U_{Th} \rangle / RP = 0.11 \text{ mJ}^{-1} \text{ extracted from the linear data fit is very close to that estimated from Ref. [10] for water drops in bulk oil } |\vec{U}_{Th}| / RP \approx 0.09 \text{ mJ}^{-1} \text{ using the order of magnitude } (\partial \sigma / \partial T) \approx 1 \text{ mNm}^{-1} \text{K}^{-1}.$$

Finally, the local thermocapillary forcing explains the slowing down followed by acceleration in the  $x$  direction observed transiently in Figure 2 when the drop front hits the beam and its rear leaves the shined region.

The beam power variation of the droplet switching efficiency is illustrated in the Inset of Figure 3 for the nine flow rate couples. It presents a very steep behavior. Below a power threshold the droplet traffic is too weakly influenced by the laser to switch direction: all drops exit from the same outlet as without laser excitation. Conversely, all droplets are deviated towards the opposite outlet above this threshold power. This threshold varies with flow rates, i.e. with  $U$  and  $R$ . Considering the drop trajectories shown in the left Inset of Figure 2, it appears that switching occurs when the mean deviation angle between the natural and the beam modified trajectory reaches some threshold value, likely related to the droplet traffic asymmetry in the  $y$  direction in the absence of laser. The tangent of this deviation can be expressed as the ratio  $\langle U_y \rangle / \langle U_x \rangle$ , where  $\langle U_x \rangle$  and  $\langle U_y \rangle$  are the drop velocities in the  $x$  and  $y$  directions, averaged over the laser-drop interaction time;  $U_x$  and  $U_y$  include both the main flow and the thermocapillary contribution. The data rescaling presented in Figure 3 shows the suspected reduction onto a single behavior. Actually, the onset  $\langle U_y \rangle / \langle U_x \rangle \approx 0.05$  corresponds to a weak mean deviation angle of  $3^\circ$  over the interaction time; this critical angle and the related beam power required for switching would be even smaller by locating the beam closer to the channel center line.

To demonstrate the reliability of laser switching for sorting droplets of different nature in lab-on-a-chips, we used the same Y-type microchannel with two upstream T junctions (seen on the left of Figure 4) instead of one. The very left one is used for the generation of pure water droplets and the other forms water/dye droplets as in the previous case. An asymmetry in outlets, designed as in Ref. 9, forces again the drops to naturally flow towards the lower outlet, whatever their composition. Since the residual optical absorption of water at  $\lambda_0 = 514.5 \text{ nm}$  is negligible ( $\approx 3 \cdot 10^{-3} \text{ cm}^{-1}$ ), pure water droplets are insensitive to the beam while water/dye droplets are spontaneously deviated and exit from the other outlet

at power above threshold. This thermocapillary sorting is illustrated in Figure 4 where water/dye and pure water droplets, produced alternatively, are shown to separate at the Y junction with *100%* efficiency.

In conclusion, we demonstrated high velocity droplet switching and sorting in microchannels based on laser-induced thermocapillary stresses. Due to the steepness variation of the switching efficiency threshold, droplets can be screened in velocity, radius and optical absorption. Moreover, the involved times scales of a few *ms* allow for digital sorting at the *kHz* range, a rate sufficient for screening reasonably large digit libraries. Finally, extension to near IR excitation would make the method even more flexible and amenable for applications since the optical absorption of pure water at  $\lambda_0 = 1500 \text{ nm}$  is  $\alpha \approx 20 \text{ cm}^{-1}$ , thus eliminating potentially polluting dyes for heating and reducing switching powers by a factor twenty. See EPAPS Ref. 15 for additional information.

The authors gratefully acknowledge the Conseil Régional d'Aquitaine for financial support (grant N° 20061102030) and the Rhodia Laboratory of Future for access to microfabrication facilities. They also wish to thank P. Pigache and E. Brasselet for experimental help, C. N. Baroud for early discussions, and J. B. Salmon for advice and technical assistance in microfabrication.

## REFERENCES

---

- <sup>1</sup> H. Song, D. L. Chen, and R. F. Ismagilov, *Angew. Chem. Int. Ed.* **45**, 7336 (2006).
- <sup>2</sup> S. L. Anna, N. Bontoux, and H. A. Stone, *Appl. Phys. Lett.* **82**, 364 (2003).
- <sup>3</sup> P. Guillot and A. Colin, *Phys. Rev. E* **72**, 066301 (2005).
- <sup>4</sup> A. Y. Fu, H. P. Chou, C. Spence, F. H. Arnold, and S. R. Quake, *Anal. Chem.* **74**, 2451 (2002).
- <sup>5</sup> D. R. Link, E. Grasland-Mongrain, A. Duri, F. Sarrazin, Z. Cheng, G. Cristobal, M. Marquez, and D. A. Weitz, *Angew. Chem. Int. Ed.* **45**, 2556 (2006).
- <sup>6</sup> K. Dholakia, M. P. MacDonald, P. Zemanek, and T. Cizmar, *Methods in Cell Biology* **82**, 467 (2007).
- <sup>7</sup> A. T. Otha, A. Jamshidi, J. K. Valley, H. Y. Hsu, and M. C. Wu, *Appl. Phys. Lett.* **91**, 074103 (2007).
- <sup>8</sup> T. H. Ting, Y. F. Yap, N. T. Nguyen, T. N. Wong, J. C. K. Chai, and L. Yobas, *Appl. Phys. Lett.* **89**, 234101 (2006).
- <sup>9</sup> K. Ahn, C. Kerbage, T. P. Hunt, R. M. Westervelt, D. R. Link, and D. A. Weitz, *Appl. Phys. Lett.* **88**, 024104 (2006).
- <sup>10</sup> K. D. Barton and R. S. Subramanian, *J. Colloid Interface Sci.* **133**, 211 (1989).
- <sup>11</sup> C. N. Baroud, J. P. Delville, F. Gallaire, and R. Wunenburger, *Phys. Rev. E* **75**, 046302 (2007).
- <sup>12</sup> E. Sloutskin, C. D. Bain, B. M. Ocko, and M. Deutsch, *Faraday Discuss.* **129**, 1 (2005).
- <sup>13</sup> Y. K. Bratukhin, K. G. Kostarev, A. Viviani, and A. L. Zuev, *Exp. Fluids* **38**, 594 (2005).
- <sup>14</sup> J. Gordon, R. C. C. Leite, R. S. Moore, S. P. S. Porto, and J. R. Whinnery, *J. Appl. Phys.* **36**, 3 (1965).
- <sup>15</sup> See EPAPS Document No. E-XXXXXXXX for two videos showing respectively drop switching (Figure 1a) and sorting (Figure 4) by local thermocapillary actuation. A direct link to this document may be found in the online article's HTML reference section. The document may also be reached via the EPAPS homepage (<http://www.aip.org/pubservs/epaps.html>) or from <ftp.aip.org> in the directory /epaps/. See the EPAPS homepage for more information.



## FIGURES

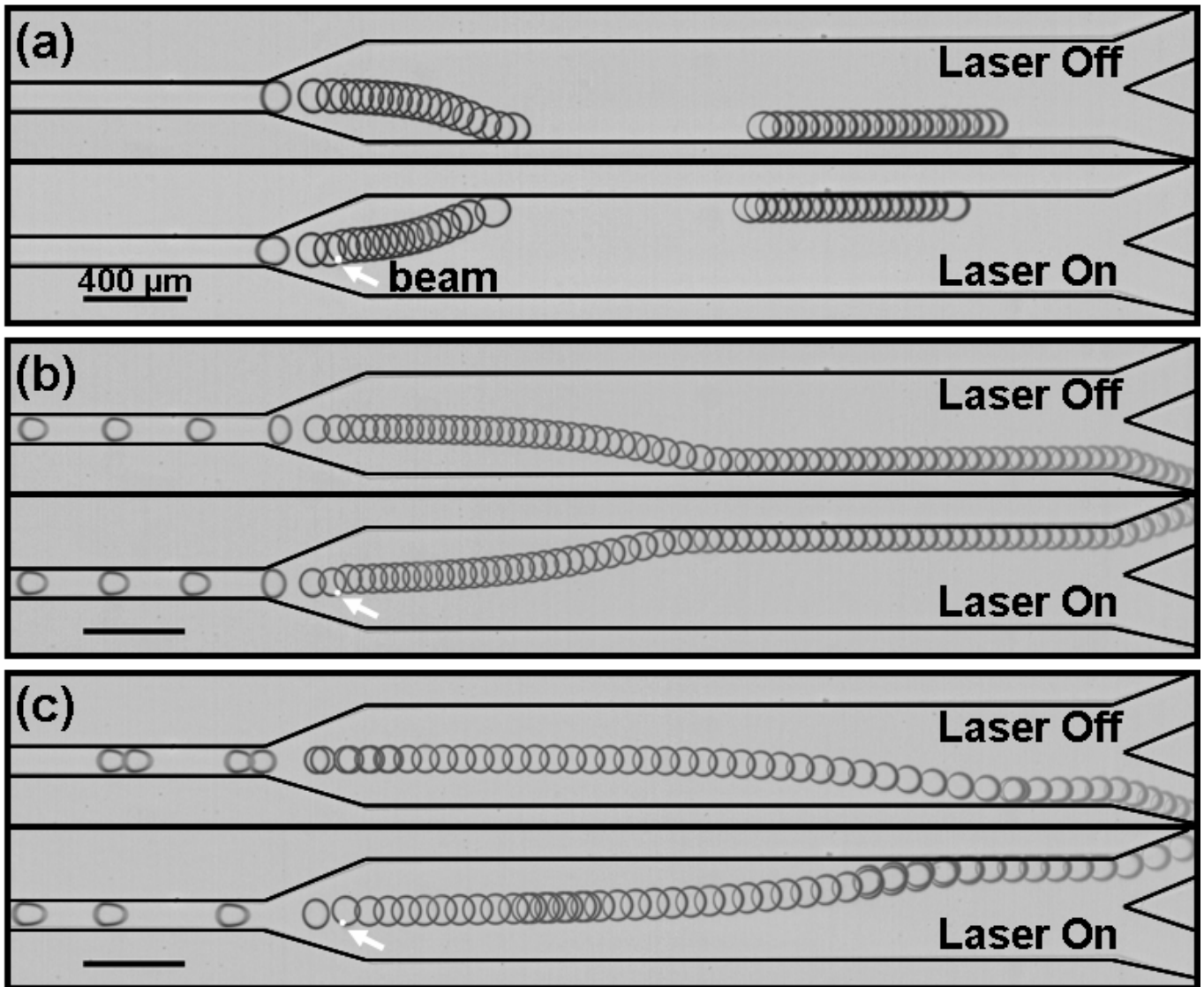


Figure 1: Superposition of successive frames illustrating drop switching by local thermocapillary actuation (frame rate  $50 \text{ fps}$ ); the arrow indicates the laser location observed by the fluorescence of the water-dye solution. a)  $Q_o/Q_w = 5/0.05$ ,  $U = 2.6 \text{ mm/s}$ ,  $R = 60 \mu\text{m}$ ,  $P = 58 \text{ mW}$ ; b)  $Q_o/Q_w = 10/0.1$ ,  $U = 6.1 \text{ mm/s}$ ,  $R = 54 \mu\text{m}$ .  $P = 111 \text{ mW}$ ; c)  $Q_o/Q_w = 15/0.2$ ,  $U = 13.0 \text{ mm/s}$ ,  $R = 55 \mu\text{m}$ .  $P = 159 \text{ mW}$ . Flow rates are expressed in  $\mu\text{l}/\text{min}$ .

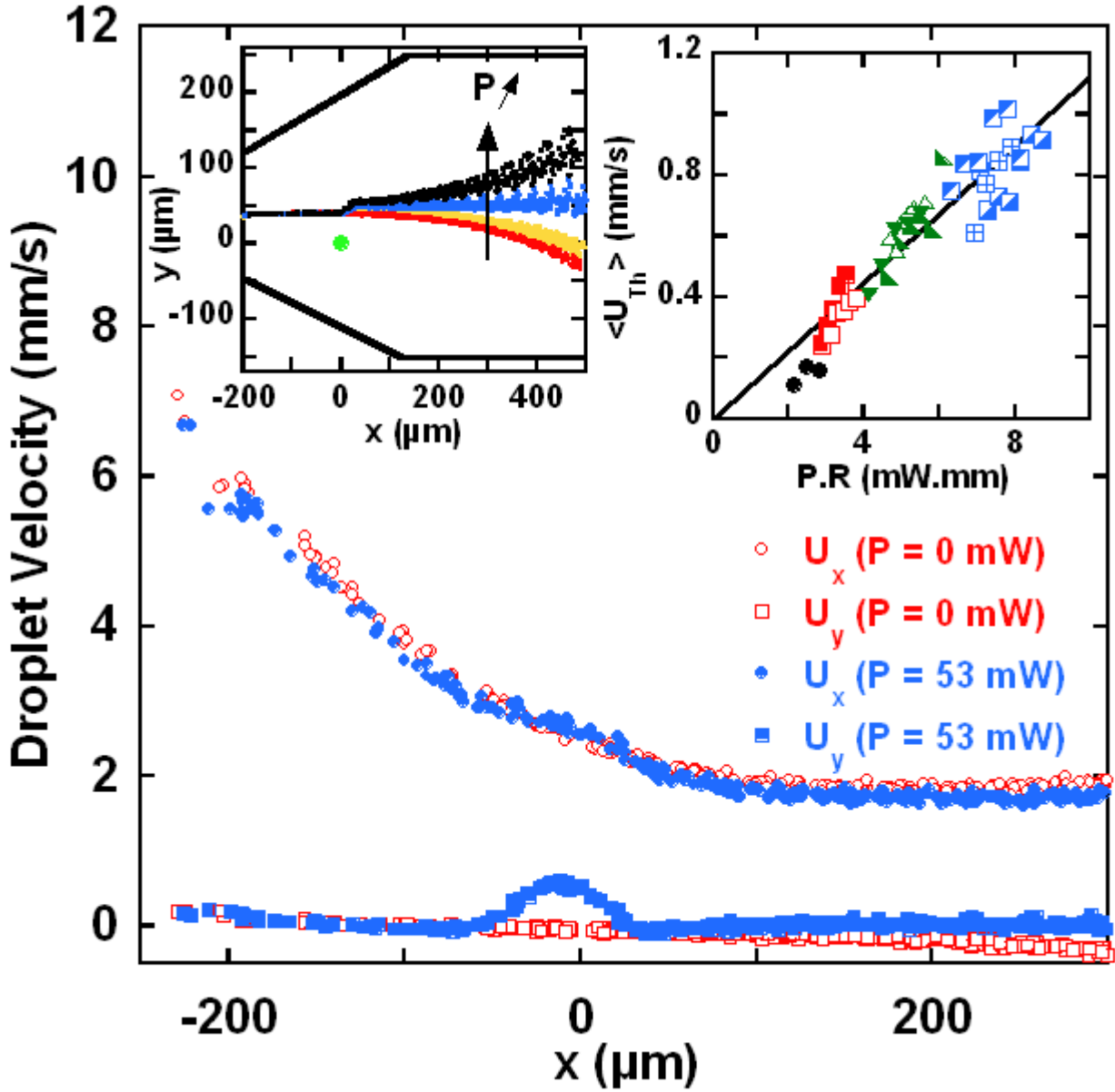


Figure 2: (Color online) Drop velocity in the  $x$  and  $y$  directions (defined in left Inset) with (filled symbols) and without (empty symbols) of laser actuation for  $Q_o/Q_w = 5/0.05$ ,  $U = 2.6 \text{ mm/s}$ ,  $R = 60 \text{ } \mu\text{m}$ ,  $P = 53 \text{ mW}$ . The main slowing down in the  $x$  direction is due to the enlargement of the Y junction. Left Inset: Trajectory of the drop center of mass for various beam powers for the same flow rates (from bottom to top:  $P = 0, 48, 53, 58 \text{ mW}$ ). The beam location is indicated by the dot at  $(x=0, y=0)$ . Right Inset: Variation of the mean drop velocity  $\langle U_{Th} \rangle$  induced by the laser beam for the nine couples of flow rates used.

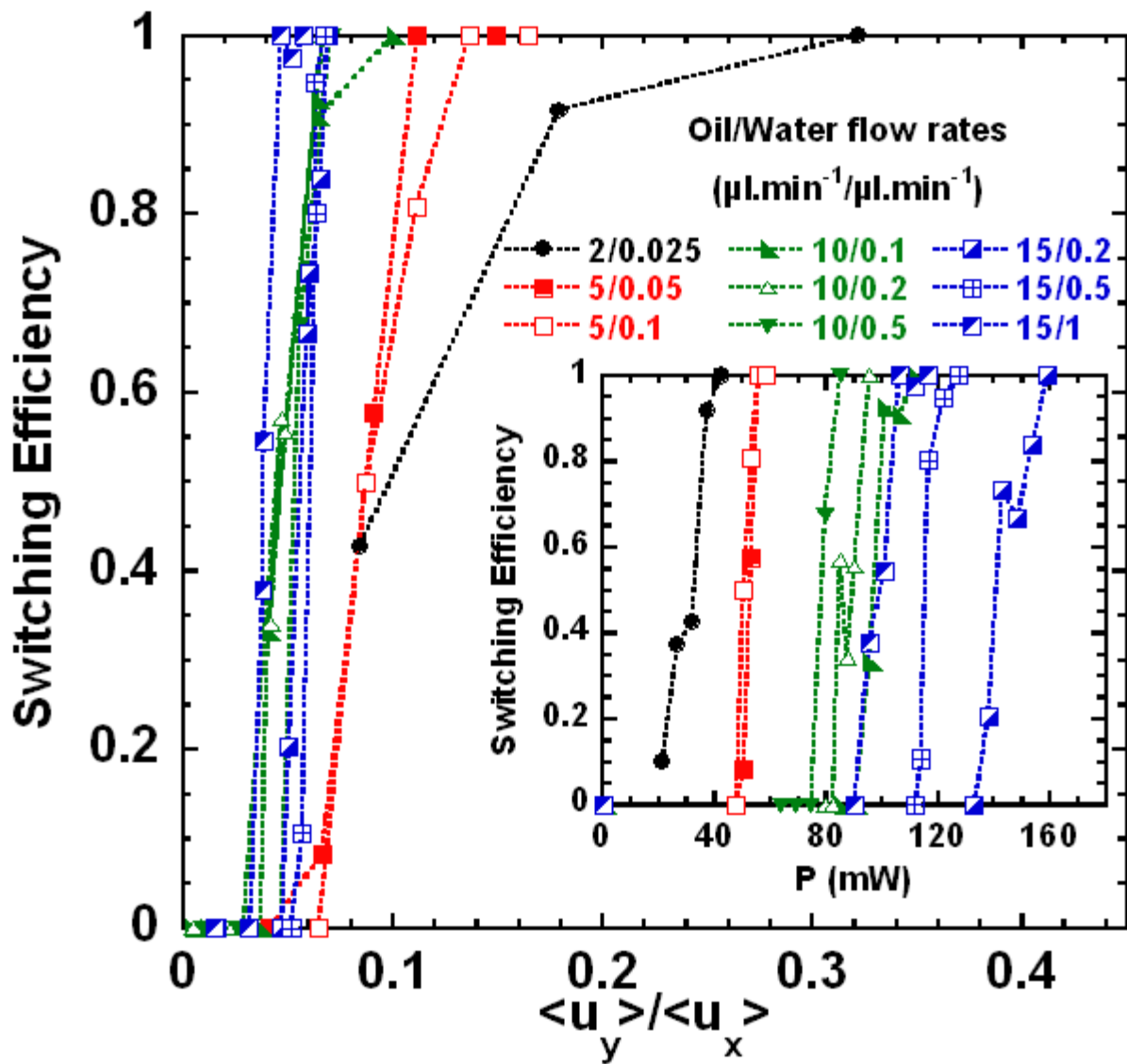


Figure 3: (Color online) Switching efficiency versus the ratio of the mean drop velocity in the  $x$  and  $y$  directions for the nine flow rate couples investigated (symbols are the same as in Figure 2). Inset: Switching efficiency plotted versus  $P$ .

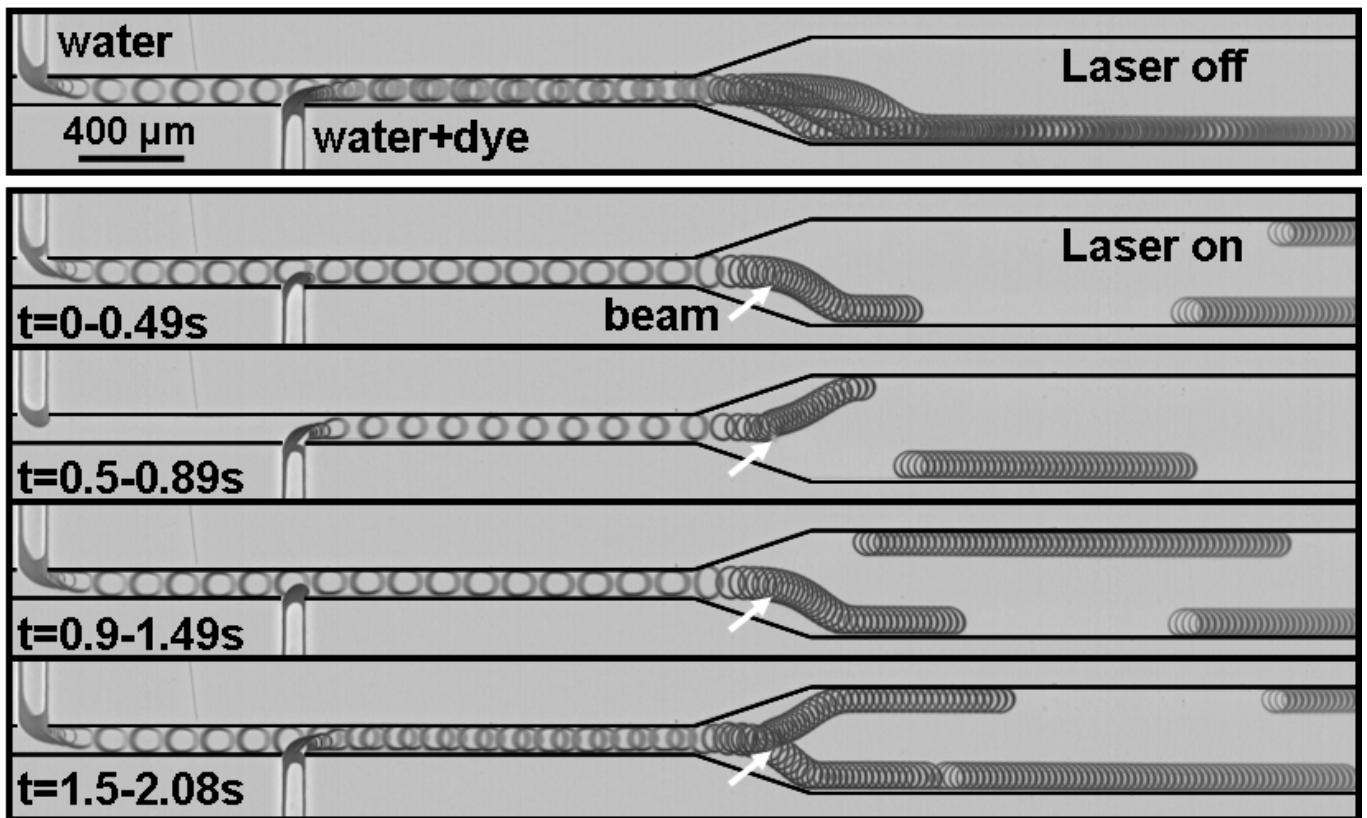


Figure 4: Sorting of pure water and water/dye droplets by local thermocapillary actuation. Top picture: superposition of 200 frames showing three drops (water/dye + water + water/dye) which are naturally drawn towards the lower outlet without laser. Bottom set: decomposition of the superposition of 209 frames when the laser shines droplets; the arrow indicates the laser location. Switching only occurs for water/dye ones ( $t = 0.5 - 0.89$  s and  $t = 1.5 - 2.08$  s where a pure water drop closely follows a water/dye one).  $Q_o/Q_w = 5/(0.03 + 0.03)$ ,  $U = 2.2$  mm/s,  $R = 59\mu\text{m}$  and  $P = 159$  mW, frame rate 100 fps.